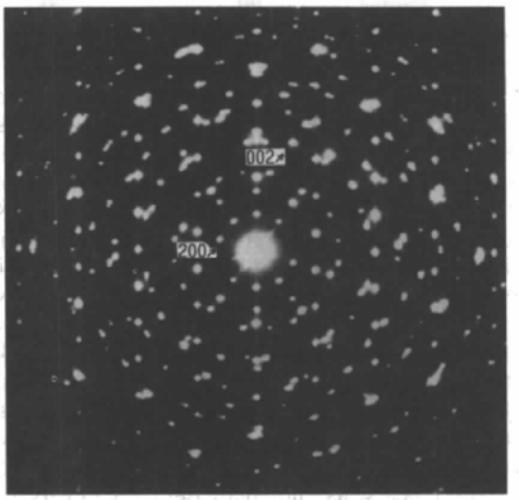

Fig. 5. Tenfold electron-diffraction pattern of the rapidly cooled alloy Fe_4Al_{13} observed by Fung, Zou & Yang (1987); reproduced courtesy of Francis & Taylor Ltd., London. Indexed are the lattice points of the high-temperature phase $Fe_4Al_{13}(h)$, $oB \sim 50$, $a^*/c^* = \tan 2\pi/5$.

The distribution of the reciprocal lattice points in Fig. 4 presumes the regular 1/5 volume share of each *oB* unit-cell orientation. Intensity irregularities observed in Fig. 5 can be explained, apart from the absorption effect, by the unequal presence of the five possible *oB* unit-cell orientations in direct space.

This work was supported by Deutsche Forschungsgemeinschaft.

References

ADAM, C. McL. & HOGAN, L. M. (1975). *Acta Metall.* **23**, 345–354.

BLACK, P. J. (1955*a*). *Acta Cryst.* **8**, 43–48.

BLACK, P. J. (1955*b*). *Acta Cryst.* **8**, 175–181.

BOUZY, E., LE CAER, G. & BAUER-GROSSE, E. (1991). *Phil. Mag. Lett.* **64**, 1–6.

BUCHER, G., ELLNER, M., SOMMER, F. & PREDEL, B. (1986). *Mh. Chem.* **117**, 1367–1378.

DAMJANOVIC, A. (1961). *Acta Cryst.* **14**, 982–987.

EDSHAMMAR, L.-E. (1964). *Acta Chem. Scand.* **18**, 2294–2302.

EDSHAMMAR, L.-E. (1965). *Acta Chem. Scand.* **19**, 2124–2130.

ELLNER, M. & BURKHARDT, U. (1993). *J. Alloys Compd.* **198**, 91–100.

FUNG, K. K., YANG, C. Y., ZHOU, Y. Q., ZHAO, J. G., ZHAN, W. S. & SHEN, B. G. (1986). *Phys. Rev. Lett.* **56**, 2060–2063.

FUNG, K. K., ZOU, X. D. & YANG, C. Y. (1987). *Phil. Mag. Lett.* **55**, 27–32.

GRIN, J., BURKHARDT, U., ELLNER, M. & PETERS, K. (1994). *Z. Kristallogr.* **209**, 479–487.

GROTH, P. (1906). *Chemische Krystallographie*, Erster Teil, pp. 47–48. Leipzig: Verlag von Wilhelm Engelmann.

HENLEY, C. L. (1985). *J. Non-Cryst. Solids*, **75**, 91–96.

HUDD, R. C. & TAYLOR, W. H. (1962). *Acta Cryst.* **15**, 441–442.

JIANG, W. J., HEI, Z. K., GUO, Y. X. & KUO, K. H. (1985). *Phil. Mag. A*, **52**, L53–L58.

LEE, J. R. (1960). *J. Iron Steel Inst.* **194**, 222–224.

LOUIS, E., MORA, R. & PASTOR, J. (1980). *Met. Sci.* **14**, 591–593.

PHILLIPS, F. C. (1971). *An Introduction to Crystallography*, 4th ed., p. 186. London: Longman.

PREDEL, B. & DUDDEK, G. (1978). *Z. Metallkd.* **69**, 773–776.

RAJASEKHERAN, T., SARAH, N. & SCHUBERT, K. (1982). *Z. Metallkd.* **73**, 526–529.

ROBINSON, K. (1952). *Phil. Mag.* **43**, 775–782.

ROBINSON, K. (1954). *Acta Cryst.* **7**, 494–497.

SALJE, E. K. H. (1990). *Phase Transitions in Ferroelastic and Co-Elastic Crystals*. Cambridge: Cambridge University Press.

SALJE, E. K. H. (1991). *Acta Cryst.* A**47**, 453–469.

SCHUBERT, K., RÖSLER, U., KLUGE, M., ANDERKO, K. & HÄRLE, L. (1953). *Naturwissenschaften*, **40**, 437.

TSUCHIMORI, M., ISHIMASA, T. & FUKANO, Y. (1992). *Phil. Mag. B*, **66**, 89–108.

ZOU, X. D., FUNG, K. K. & KUO, K. H. (1987). *Phys. Rev. B*, **35**, 4526–4528.

Acta Cryst. (1995). B**51**, 36–43

A Family of τ-Inflated Monoclinic $Al_{13}Co_4$ Phases

BY X. L. MA, X. Z. LI AND K. H. KUO*

Beijing Laboratory of Electron Microscopy, Chinese Academy of Sciences, PO Box 2724, 100080 *Beijing, People's Republic of China*

(*Received* 25 *June* 1994; *accepted* 30 *August* 1994)

Abstract

Monoclinic τ^2-$Al_{13}Co_4$, τ^3-$Al_{13}Co_4$ and τ^4-$Al_{13}Co_4$ phases with a and c parameters about τ^2, τ^3 and τ^4 times [$\tau = (1 + 5^{1/2})/2 = 1.61803$, which is the golden number], respectively, greater than their counterparts in $Al_{13}Co_4$ (space group Cm, $a = 1.5183$, $b = 0.8122$, $c = 1.2340$ nm, $\beta = 107°54'$ [Hudd & Taylor (1962). *Acta Cryst.* **15**, 441–442]) have been found by selected-area electron diffraction and high-resolution electron

* Please send all correspondence to Dr K. H. Kuo, PO Box 2724, 100080 Beijing, People's Republic of China.

microscopy (HREM). The [010] HREM images showed that these τ-inflated phases have a similar pentagonal layer structure as $Al_{13}Co_4$, but the edge length of the pentagons is τ^2, τ^3 and τ^4 times larger, respectively, than that in $Al_{13}Co_4$. This explains why these τ-inflated phases have about the same β angle ($\simeq$108°) and b representing a repeat unit of the stacking of these pentagonal layers. The τ^2 pentagon (1.23 nm) consists of six smaller pentagons (0.47 nm) existing in $Al_{13}Co_4$, one inverted and five of the same orientation as the τ^2 pentagon. Similarly, the τ^3 pentagon (2.00 nm) consists of six τ pentagons (0.76 nm), and the τ^4 pentagon (3.23 nm) of six τ^2 pentagons which in turn contain six 0.47 nm pentagons in each of them. The greater the inflation, the larger the unit-cell parameters, and the better the approximation of its structure to that of a decagonal quasicrystal (DQC). In other words, a DQC is considered to be the end member of this family of τ-inflated phases.

1. Introduction

In a study of the crystalline and quasicrystalline phases in binary Al–Co alloys, Ma & Kuo (1992) found a primitive as well as a C-centred monoclinic τ^2-$Al_{13}Co_4$ phase whose a and c parameters are about τ^2 times [$\tau = (1 + 5^{1/2})/2 = 1.61803$, which is the golden number] greater than those in $Al_{13}Co_4$, but their b parameter and β angle ($\simeq$108°) remain about the same. These τ^2-$Al_{13}Co_4$ phases were found to coexist with the Al–Co decagonal quasicrystal (DQC) which is periodic along the tenfold axis but quasiperiodic in the plane normal to this axis. Moreover, the binary Al–Co DQC with the composition of $Al_{13}Co_4$ was a stable phase between 1073 and 1173 K, and the crystalline τ^2-$Al_{13}Co_4$ can transform to a DQC and *vice versa* by a change of temperature (Ma & Kuo, 1994). The strong diffraction spots in the [010] electron-diffraction pattern (EDP) of τ^2-$Al_{13}Co_4$ form many pentagons and decagons resembling the tenfold EDP of a DQC. It was suggested that both τ^2-$Al_{13}Co_4$ and the Al–Co DQC consist basically of the same pentagonal subunit inflated τ^2 times from that in $Al_{13}Co_4$, packed periodically in the crystalline phases and aperiodically in the DQC. This supposition was proved in this study by high-resolution electron microscopy (HREM) since the Co atoms can be imaged as bright points forming pentagons (edge length 0.47 and 1.23 nm) and the arrangement of these pentagons can be studied in detail. Such a study has also been extended to two new monoclinic phases with a and c parameters about τ^3 and τ^4 times, respectively, greater than those in $Al_{13}Co_4$. The pentagon subunits in the τ^3-$Al_{13}Co_4$ phase are also of two sizes, 0.76 and 2.00 nm, and those in the τ^4-$Al_{13}Co_4$ phase are 1.23 and 3.23 nm, respectively. It is of interest to note that the edge lengths of pentagons, 0.47, 0.76, 1.23, 2.00 and 3.23 nm, are approximately in τ-inflated ratios, $1 : \tau : \tau^2 : \tau^3 : \tau^4$. These numbers are not only geometric but also additive, *i.e.* $\tau^2 = \tau + 1$, $\tau^3 = \tau^2 + \tau$, *etc.*

The τ^2-inflation can best be understood with a description of the pentagram, Fig. 1. Extending the edges of a unit pentagon ABCDE, a pentagonal star with apicies at F, G, H, I, J results. Since the length of a diagonal, *e.g.* AC, of this unit pentagon is τ and CH = AC, line JH is divided into three irrational segments with length ratios τ:1:τ. Connecting these apicies, a large, inverted pentagon FGHIJ will result, and its edge length HI = HD = $1 + \tau = \tau^2$. Within this τ^2-inflated pentagon FGHIJ, there are one small, inverted pentagon ABCDE at the centre and another five small pentagons surrounding the central one. In addition, there are five isosceles triangles or rather five halves of 36° rhombi (drawn in dotted lines). If such inflation continues, a τ^4-inflated pentagon appears, as shown in Fig. 1. Conversely, the unit pentagon ABCDE can also deflate, and an inverted pentagon with an edge length of τ^{-2} appears at its centre, Fig. 1. Thus, it becomes clear that this τ^2inflation/deflation process can repeat infinitely.

The structures of $Al_{13}Co_4$ and $Al_{13}Fe_4$ are basically the same. Owing to the loss of the inversion centre, the space group changes from $C2/m$ in $Al_{13}Fe_4$ (Black, 1955*a*) to Cm in $Al_{13}Co_4$ (Hudd & Taylor, 1962). These two monoclinic $Al_{13}M_4$ ($\beta \simeq 108°$) phases have a pentagonal layer structure. In the (010) layer at $y = 0$ and $\frac{1}{2}$, the M atoms form a network of pentagons and 36° rhombi with an edge length of 0.47 nm, see the solid circles in Fig. 2(*a*). The diagonal of a pentagon is about $0.47\tau = 0.76$ nm. As shown in Fig. 2(*a*), the parameter a roughly equals two diagonals, *i.e.* 1.52 nm, and the parameter c is equal to one edge plus one diagonal, *i.e.* 1.23 nm. These values compare favourably with the experimentally determined lattice parameters of $Al_{13}Co_4$, $a = 1.5183$ and $c = 1.2340$ nm (see Table 1). The M atoms in the puckered layers at about $y \simeq \frac{1}{4}$ and $\frac{3}{4}$ fall at the centres of these pentagons (shown as open circles in

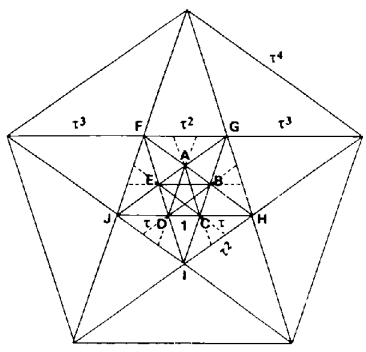

Fig. 1 A pentagram showing the τ^2 inflation/deflation of pentagons. The separations between vertices on a line are in $1:\tau:\tau^2:\tau^3 : \ldots$ irrational ratios. Within the τ^2-inflated pentagon FGHIJ, there are one inverted small pentagon ABCDE at the centre and five more surrounding it (drawn in dotted lines).

Table 1. Lattice parameters and the pentagonal layer of the τ-inflated $Al_{13}Co_4$ phases

Phases	Lattice parameters a (nm)	b (nm)	c (nm)	β (°)	Pentagon (nm)
$Al_{13}Co_4$	1.5183	0.8122	1.2340	107.90	0.47
τ-$Al_{13}Co_4$					0.76
τ^2-$Al_{13}Co_4$	3.984	0.8148	3.223	107.94	1.23
τ^3-$Al_{13}Co_4$	6.4	0.81	5.2	108	2.00
τ^4-$Al_{13}Co_4$	10.4		8.4	108	3.23

τ^∞-$Al_{13}Co_4$ Decagonal quasicrystal.

Fig. 2*a*). The Al atoms in the puckered layers surrounding the Co atoms form pentagons of 0.29 nm, *i.e.* τ times smaller than 0.47 nm. The distribution of Al atoms in the flat layer in the left half of the unit cell is different from the right half. Henley (1985) and Kumar, Sahoo & Athithan (1986) considered the pentagonal layer structure of the monoclinic $Al_{13}Fe_4$ as the prototype structure of a DQC. Recently, Barbier, Tamura & Verger-Gaugry (1993) discussed the pseudo-icosahedral coordination in $Al_{13}Fe_4$ as a link between icosahedral and decagonal quasicrystals. Steurer & Kuo (1990) found experimentally part of the $Al_{13}Co_4$ unit cell in the structure of an Al–Co–Cu DQC. Since the τ-inflated τ^2-, τ^3- and τ^4-$Al_{13}Co_4$ show more resemblance to a DQC, a detailed study of their layer structures will certainly shed some light on the understanding of the structure of a DQC and the related monoclinic $Al_{13}Co_4$ phases with τ-inflated unit cells. This was carried out mainly by HREM.

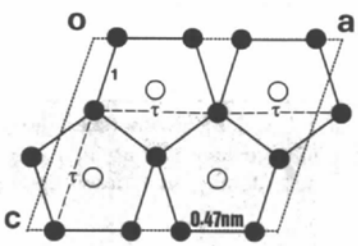

(*a*)

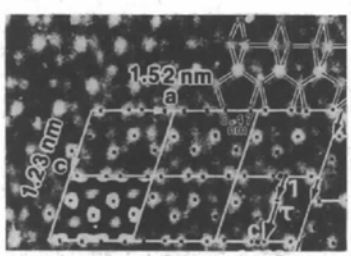

(*b*)

Fig. 2 (*a*) The projection of Co-atom pentagonal layers in $Al_{13}Co_4$: $y = 0$ and $\frac{1}{2}$, solid circles: $y \simeq \frac{1}{4}$ and $\frac{3}{4}$, open circles. *a* roughly equals two diagonals whereas *c* is one edge plus one diagonal. (*b*) [010] HREM image with bright image points forming centred pentagons and 36° rhombi corresponding to the Co atoms in (*a*). A simulated image from Fig. 3(*b*) is patched on the lower left-hand projected unit cell.

2. Experimental

Binary alloys of nominal compositions varying between $Al_{13}Co_4$ and $Al_{10}Co_4$, each about 600 g, were made by melting high-purity metals in alumina crucibles in an induction furnace. Alloy samples were heat treated at temperatures from 973 to 1223 K in sealed and evacuated silica tubes. Thin-foil specimens for transmission-electron microscopic observations were prepared by slicing, grinding and ion-milling. A Philips EM420 electron microscope working at 100 kV was used for electron-diffraction experiments, whereas a JEM 2010 electron microscope with a point resolution of 0.194 nm working at 200 kV was used for HREM.

Fig. 2(*b*) shows the observed [010] HREM image of $Al_{13}Co_4$, in which some unit cells are outlined. The pentagons in these unit cells are marked with black dots and some pentagons above them are outlined. However, the image points at the pentagon centres are diffuse and often not at the exact centre. This HREM image agrees in general with the pentagonal distribution of Co atoms shown in Fig. 2(*a*). Tsuchimori, Ishimasa & Fukano (1992) have made an HREM study of $Al_{13}Fe_4$ and found bright image points in an (010) image forming centred pentagons of edge length 0.47 nm, similar to Fig. 2(*b*). This is quite natural since the structures of these two $Al_{13}M_4$ phases are almost the same.

For comparison purposes, simulated HREM images of $Al_{13}Co_4$ were calculated using a multi-slice program written by Dr Y. M. Chu from this laboratory specially for an AST 486 PC. The electron optical parameters are: spherical abberation coefficient, $Cs = 0.5$ mm, defocus values varying from -10 to -80 nm, condenser aperture 200 μm and spot size 150 nm. The thickness of 20 nm is divided into 100 slices. Fig. 3 shows the simulated HREM images for a thickness of 20 nm at various underfocus values. Obviously, the image contrast varies materially within this defocus range, and the image at a defocus value of -20 nm gives the best fit with the observed image shown in Fig. 2(*b*). A unit cell is cut from Fig. 3(*b*) and patched on the lower-left oblique cell in Fig. 2(*b*). By tilting either the electron beam or the foil orientation, the image point at the pentagon centre becomes diffuse and is also shifted from its central position. In the case of thin foils a few tens of nanometres thick, local buckling cannot always be avoided. This makes the shift of the central image points random in the observed HREM image. From this comparison of observed and simulated HREM images, it becomes clear that HREM images can possibly be used to show the characteristic distribution of Co atoms in this kind of layer structures.

3. Electron diffraction

After solidification both crystalline and quasicrystalline phases were present in these alloys. However, DQC was

found stable only within 1073–1173 K (Ma & Kuo, 1994). After heating to 1223 K followed by water quenching, the main crystalline phase is the primitive τ^2-$Al_{13}Co_4$ with many thin twin lamellae in it, although sometimes some τ^3-$Al_{13}Co_4$ and τ^4-$Al_{13}Co_4$ domains of several nanometers in size can also be found. In general, the main phase can easily be identified by X-ray powder-diffraction analysis. However, owing to the rather large lattice parameters of the τ^2-$Al_{13}Co_4$ phase (see Table 1), the indexing of a powder diffractogram becomes a difficult task (for the indexing of τ^2-$Al_{13}Co_4$, see Ma & Kuo, 1994). Therefore, selected-area electron diffraction was mainly used to identify these phases in the present study.

Fig. 4 shows a composite EDP of the [010] EDP's of the *C*-centred $Al_{13}Co_4$ (*a*), the primitive τ^2-$Al_{13}Co_4$ (*b*), and the primitive τ^3-$Al_{13}Co_4$ (*c*), as well as the tenfold EDP of the coexisting Al–Co DQC (*d*). In Fig. 4(*d*), the diffraction spots not only have a tenfold distribution but their distribution along a row also follows the irrational τ-inflation relationship, *i.e.* in $1{:}\tau{:}\tau^2{:}\tau^3$ ... ratios. On the other hand, the diffraction spots in Figs. 4(*a*)–4(*c*) all fall on a crossgrid, although the sizes of these meshes are different. The corresponding diffraction spots in these EDP's were marked with black and white arrowheads, respectively. The spots marked with black arrowheads in Fig. 4(*a*)–4(*c*) have the $|l|$ indices 5, 13 and 21, respectively, and those with white arrowheads the $|h|$ indices 6, 16 and 26, respectively. The ratios of these numbers following the Fibonacci series (0, 1, 1, 2, 3, 5, 8, 13, 21, ...) are approximately in $1{:}\tau^2{:}\tau^3$ inflation. The $h0l$ reflections with h odd are forbidden owing to *C*-centring in Fig. 4(*a*). However, these reflections appear in Figs. 4(*b*) and 4(*c*) since the τ^2- and τ^3-phases are no longer *C*-centred. The oblique ($\beta^* \simeq 72°$) reciprocal cells in these EDP's are, therefore, deflated by approximately $1{:}\tau^{-2}{:}\tau^{-3}$ ratios. The ten strong spots on the outer ring are marked with black dots. They form almost a perfect decagon, no matter whether they belong to a DQC or to different crystalline phases. Moreover, the rows of strong spots in the DQC in Fig. 4(*d*) pass continuously into those of the τ^3-inflated phase in Fig. 4(*c*). The corresponding spots forming a pentagon in Fig. 4(*d*) and pseudo-pentagons in Figs. 4(*b*) and 4(*c*) are indicated by arrows. Inside them, there is a τ^{-2}-deflated pentagon in Fig. 4(*d*), a pseudo-pentagon in Fig. 4(*c*), and a rather deformed pentagon in Fig. 4(*b*). All these diffraction spots are marked with dots. In Fig. 4(*d*), there is even a τ^{-4}-deflated pentagon resembling the pentagram shown in Fig. 1, but not in the other two EDP's. The similarity between the tenfold distribution of diffraction spots in a DQC and that of the strong spots in the family of τ-inflated phases increases with the order of τ inflation or the unit-cell size. In this context, the DQC may be considered as the end member of this inflation series with an infinitely large unit cell.

The lattice parameters of these τ-inflated $Al_{13}Co_4$ phases are shown in Table 1. Those for $Al_{13}Co_4$ (Hudd & Taylor, 1962) and τ^2-$Al_{13}Co_4$ (Ma & Kuo, 1994) are obtained by X-ray diffraction methods, whereas those for

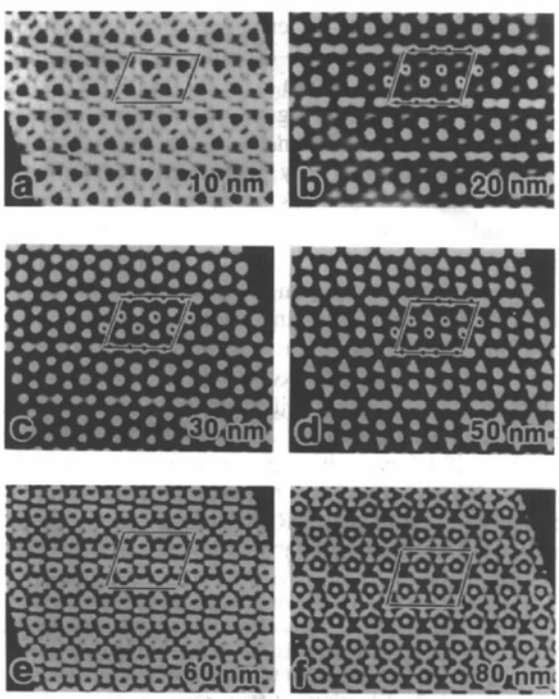

Fig. 3 Simulated [010] HREM image for a thickness of 20 nm and various underdefocus values. The defocus value at −20 nm gives the best fit with the observed HREM image shown in Fig. 2(*b*).

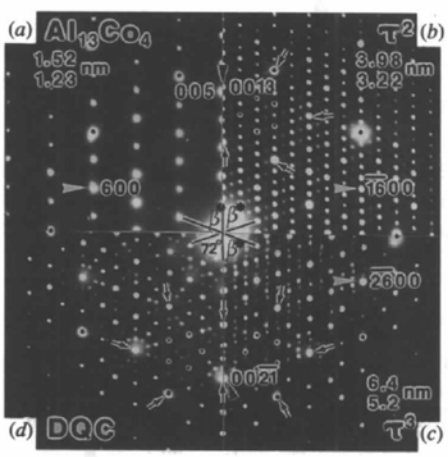

Fig. 4. A composite EDP of the [010] EDP's of the monoclinic $Al_{13}Co_4$ (*a*), the τ^2-inflated phase (*b*), and the τ^3-inflated phase (*c*), as well as the tenfold EDP of the Al–Co DQC (*d*). Arrows, arrowheads and dots show the corresponding diffraction spots in these EDP's. The greater the inflation, the larger the unit-cell parameters, and the closer the approximation of a τ-inflated phase to the DQC. Note straight spot-rows passing almost continuously from (*d*) into (*c*) and the concentric pentagons in them indicated by arrows and dots.

τ^3-$Al_{13}Co_4$ by electron diffraction. For τ^4-$Al_{13}Co_4$, the domain size is too small to take a selected-area EDP. In this case, the lattice parameters are estimated from the HREM image. The lattice parameter $b \simeq 0.81$ nm of the τ^3-inflated phase is determined from an EDP containing the $0k0$ diffraction spots and is equal to the periodicity along the tenfold axis of a DQC. The edge lengths of the pentagons in these τ-inflated phases are also shown in Table 1. They are also in τ-inflated ratios.

4. High-resolution electron microscopy

4.1. τ^2-$Al_{13}Co_4$

Fig. 5(*a*) is the HREM image taken along the **b** axis of τ^2-$Al_{13}Co_4$ showing bright image points forming pentagons of two different sizes. The large pentagons are marked with solid circles, whereas some of the small centred pentagons are marked with dots. The oblique plane cells are indicated by octagonal stars and the lower left one corresponds to the schematic illustration shown in Fig. 5(*b*). The small centred pentagons with an edge length of 0.47 nm are the same as those observed in $Al_{13}Co_4$ but in a different tessellation compared with Fig. 2(*a*). In a large pentagon of edge length 1.23 nm, there are six small pentagons, one inverted at the centre and five of the same orientation as the large one surrounding the central small pentagon, see also Fig. 1. It is of interest to note that the tessellation of the large pentagons of τ^2-$Al_{13}Co_4$ in Fig. 5 is exactly the same as the small pentagons of $Al_{13}Co_4$ in Fig. 2. In addition to the pentagon of edge length of 1.23 and 0.47 nm, there are also pentagons of 0.76 and 0.29 nm (marked with a pentagonal star at their common centre), also in inverted orientation and in τ^2 inflation/deflation. The Co-atom pentagons of egde lengths 0.29, 0.47, 0.76 and 1.23 nm form a τ-inflated series. They form two τ^2-inflation series: one is 0.47, 1.23, 3.23 ..., and the other is 0.29, 0.76, 2.00 ... . The image points around the vertices of the 1.23 nm pentagons form concentric decagons, see that marked with *V* in Fig. 5 and those at the bottom right-hand corner of Fig. 5(*b*). In other words, the decagonal nature of this τ^2-inflated phase becomes obvious. This will be discussed further in §4.4.

4.2. τ^3-$Al_{13}Co_4$

Fig. 6 shows the τ^3-inflated phase with pentagons (also marked with solid circles) of edge length 2.0 nm. Inside these pentagons there are τ^{-2}-deflated ones (0.76 nm) marked with dots. Their distribution is the same as those small pentagons (0.47 nm) in the large ones (1.23 nm) in the τ^2-inflated phase shown in Fig. 5. In addition, there are also pentagons of edge length 0.47 and 1.2 nm, as shown in the upper left-hand corner in Fig. 5. It is of interest to note that the two outlined unit cells are in glide-reflection symmetry, see the pentagons or even better the outlined thin rhombi across the twin boundary indicated by arrowheads. The glide component indicated by an arrow is one half of the diagonal of the large pentagon, or $\frac{1}{2}\tau c/(1+\tau) = 0.31c$. Such a (100) glide-twin relationship in $Al_{13}Fe_4$ has been discussed earlier by Black (1955*b*) and recently studied by HREM (Tsuchimori *et al.*, 1992). The observation made on the τ^3-inflated phase not only confirms this glide-twin relationship but also shows the similarity in twin formation in the τ-inflated phases. In addition to the (100) glide twins, (001) and (−201) glide twins have also been found in τ^2-$Al_{13}Co_4$ and a combination of these will result fivefold twins (Ma & Kuo, 1995).

4.3. τ^4-$Al_{13}Co_4$

Fig. 7 shows the HREM image of the τ^4-inflated phase whose unit cell is indicated by arrowheads. Again there is pentagonal network similar to that in $Al_{13}Co_4$, the τ^2- or the τ^3-inflated phase, but the edge length of pentagons is 3.23 nm, or τ^4-inflated of 0.47 nm. Such a pentagon consists of six pentagons of edge length 1.23 nm, one

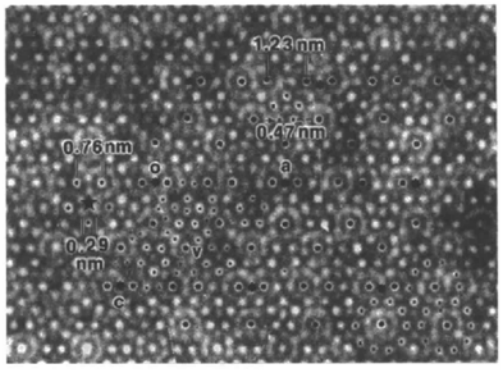

(*a*)

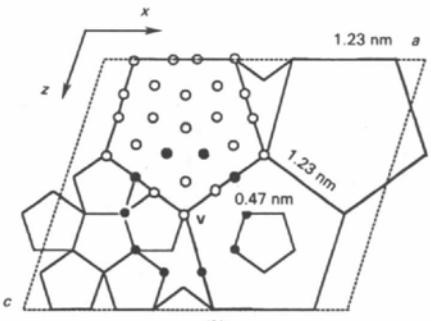

(*b*)

Fig. 5. (*a*) [010] HREM image showing the pentagonal network in the τ^2-inflated phase, similar to that in Fig. 2(*b*) but τ^2 times inflated. The oblique plane cells are outlined with octagonal stars. Around the vertices of this 1.23 nm pentagon (marked with solid circles) there are concentric decagons of bright image points, see that marked V and those at the bottom right-hand corner. There are also pentagons of 0.29 and 0.76 nm (marked with a pentagonal star) in the τ-inflated series. A schematic diagram of the lower left-hand unit cell giving the Co-atom sites is shown in (*b*).

inverted in the centre and five of the same orientation as the large pentagon. Within this small pentagon, there are six even smaller pentagons of edge length 0.47 nm. Such τ^4-$Al_{13}Co_4$ unit cells have only been observed in isolated cases. The a and c parameters of this τ^4-inflated phase measured from Fig. 7 are 10.4 and 8.4 nm, respectively. This is the largest monoclinic unit cell ($\beta \simeq 108°$) ever found coexisting with a DQC.

4.4. τ^2-$Al_{13}Co_4$ → *DQC transition*

Fig. 8 is an aperiodic Penrose pattern displaying local fivefold symmetry taken from *Tiling and Patterns* (Grünbaum & Shephard, 1987), originally invented by Penrose (1974). After the discovery of quasicrystals, especially the DQC's, the Penrose pattern was used extensively to describe the two-dimensional tenfold quasilattice. There are three equivalent sets of Penrose tiles. Set 1 consists of four kinds of Penrose tiles (for the present, observe only those tiles in thin lines): pentagons, thin (36°) rhombi, stars and boats (marked with a small B in Fig. 8), all having angles in multiples of $\pi/5$. According to a set of rigorous matching rules, these tiles can form an infinite aperiodic pattern. Very often three pentagons, two rhombi and one boat form a decagon. Both Penrose tiles and the decagons can inflate by $1 + \tau = \tau^2$ times, see the tiles in thick lines in Fig. 8. A small boat will inflate to a large boat (marked large B), a small decagon to a large decagon, *etc*. Of course, the Penrose tiles can also deflate by τ^{-2} times. The τ^2 inflation/deflation can proceed infinitely.

The inflation of a small pentagon to a large pentagon in Fig. 8 deserves special attention, because it reminds the configuration of six small pentagons of $Al_{13}Co_4$ (edge length 0.47 nm) in a large pentagon of τ^2-$Al_{13}Co_4$ in Fig. 5. These large pentagons are packed periodically in this crystalline phase but aperiodically in a DQC.

Between the τ^2 phase and a DQC, there might be a transition region. In order to test this supposition, an alloy sample of the composition of $Al_{13}Co_4$ was heated to 1223 K and cooled in air, so that part of the τ^2-$Al_{13}Co_4$ phase existing at this temperature was transformed partially to DQC during cooling through the temperature range 1073–1173 K, where DQC is the stable phase (only quenching in water can prevent this transformation). Fig. 9 is an [010] HREM image showing this transitional structure. In the present case, the foil is not so thin so that the resolution of this HREM image is not as good as that of Fig. 5. However, this might not be a disadvantage since only the pentagons as a whole are of interest. The central small pentagon with an edge length of 0.47 nm shows a dark contrast, which makes the identification of the large pentagons of edge length 1.23 nm much easier. This greatly facilitates the analysis of the aperiodical arrangement of these pentagons. On the left, only the τ^2-$Al_{13}Co_4$ phase exists and one unit cell consisting of pentagons and rhombi (edge length

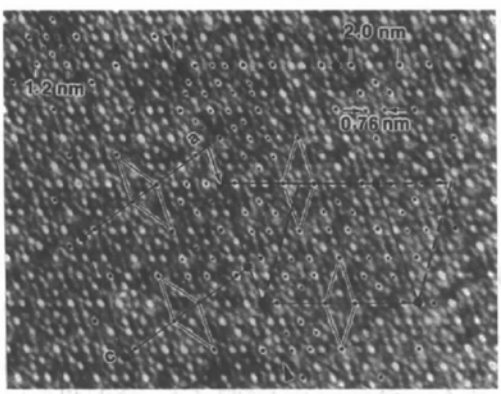

Fig. 6. [010] HREM image showing two unit cells of the τ^3-inflated phase in (100) glide-reflection twin relation. The glide component (indicated by an arrow) is $0.31c$. Compare the outlined thin rhombi and pentagons marked with dots in these two unit cells. The 2.0 nm pentagons are marked by small solid circles.

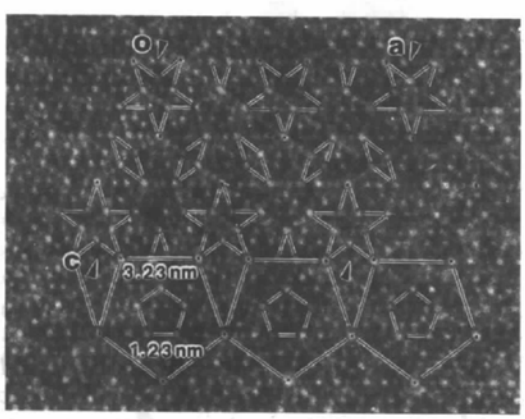

Fig. 7 [010] HREM image showing a giant unit cell of the τ^4-inflated phase. Some of the 3.23 nm pentagons and the central 1.23 nm pentagons in them are outlined at the bottom.

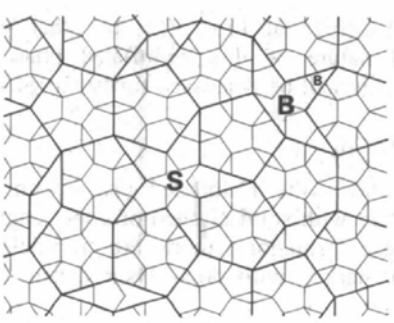

Fig. 8. The Penrose pattern consists of an aperiodic arrangement of pentagons, 36° rhombi, boats (marked B), and stars (marked S), taken from Grünbaum & Shephard (1987). The tiles drawn with thick lines are τ^2-inflated from the tiles of thin lines. Note the large pentagon containing six small pentagons is exactly the same as in the τ^2-$Al_{13}Co_4$ phase shown in Fig. 5.

1.23 nm) identical to those shown in Fig. 5 is outlined. The other rhombi in this region are also outlined to show their uniform orientation and periodical arrangement. This also shows a uniform and periodical arrangement of the 1.23 nm pentagons. To the right of this crystalline region thin rhombi of different orientations begin to appear, and a boat sometimes appears between two rhombi differing by 36° in orientation. Gradually, boats increase in number and finally a star S appears at the bottom right-hand corner of Fig. 9. Altogether there are four differently oriented rhombi and three differently oriented boats. Such a configuration of pentagons, rhombi, boats and stars implies a development of aperiodic order in a periodic matrix. In other words, this is the beginning of the transition from a crystalline phase to a DQC. The presence of some rhombi and boats with the same orientation in this aperiodic region can be considered as phason defects in a DQC.

5. Concluding remarks

(1) The presence of a family of monoclinic phases with the same $\beta \simeq 108°$ and b [or the same stacking sequences of the (010) pentagonal layers] as the prototype structure of $Al_{13}Co_4$, but a and c parameters τ^2, τ^3 and τ^4 times larger, where $\tau = (1 + 5^{1/2})/2$ is the golden number associated with tenfold/fivefold symmetry [cos 36° = $\tau/2$, cos 72° = $(\tau - 1)/2$], shows on the one hand the close structural relationship of these phases among themselves and on the other hand their close structural relationship to the decagonal qausicrystals characterized by the irrational τ. High-resolution electron microscope (HREM) images of the (010) pentagonal layers of these phases make it clear that their τ-inflated lattice parameters are caused by a τ-inflation of the Co-atom pentagons of edge length 0.47 nm in $Al_{13}Co_4$, but the tessellation of these pentagons remains the same. This inflation process can proceed infinitely, and a decagonal quasicrystal might be considered as the end member of this inflation series so that its unit cell becomes infinitely large.

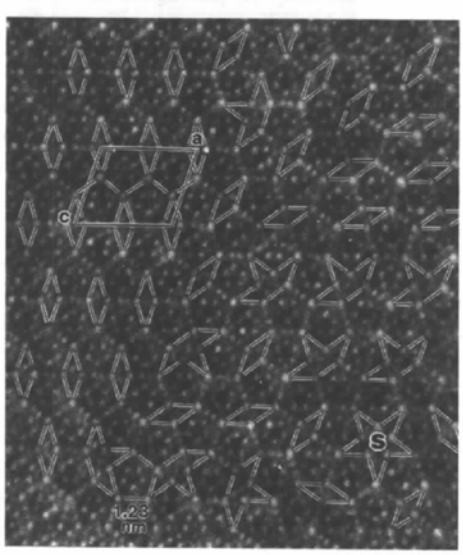

Fig. 9. [010] HREM image showing the growth of aperiodic order in the τ^2-$Al_{13}Co_4$ phase. On the left part, the rhombi and also the pentagons show a periodic arrangement with a uniform orientation (one unit cell is outlined). Gradually rhombi with different orientations begin to appear, and boats occur between two rhombi with a difference of 36° in orientation. Finally, a star S surrounded by pentagons appears at the bottom right-hand corner.

(2) The pentagonal layer of these τ-inflated phases consists of a network of pentagons and 36° rhombi, and the latter can possibly be visualized as the intervening spaces left by the pentagons. Among these τ-inflated phases, the τ^2-$Al_{13}Co_4$ phase occurs most frequently and abundantly. The pentagon in this phase has an edge length of 1.23 nm and consists of six smaller pentagons of 0.47 nm, one inverted in its centre and the other five surrounding the central one. This is of interest in two respects: first, such a configuration of pentagons of two different sizes also occurs in the celebrated Penrose pattern (Penrose, 1974), which has been extensively used as a quasilattice model for the two-dimensional decagonal quasicrystals. Second, an aperiodic tessellation of pentagons, rhombi, boats and stars, known as Penrose tiles, with an edge length of 1.23 nm has been observed in the HREM images of an Al–Co–Cu decagonal quasicrystal (Li, Zhang & Kuo, 1994). In the present study, an intermediate stage between the crystalline τ^2-$Al_{13}Co_4$ and quasicrystalline phases has been observed. The uniformly oriented and periodically distributed pentagons in τ^2-$Al_{13}Co_4$ gradually become disoriented and aperiodic, and the Penrose tiles, boats and stars begin to appear. From the tiling point of view, it might be suggested that a quasicrystal and a related crystalline phase consist of almost the same pentagonal structural units, tiled aperiodically in a quasicrystal and periodically in a crystal. In fact, part of the unit cell of the monoclinic $Al_{13}Co_4$ can be found in the structure of the Al–Co decagonal quasicrystal (Steurer & Kuo, 1990). It should be pointed out that both quasicrystalline and crystalline phases have been found earlier in an Al–Co–Cu alloy by Hiraga, Sun & Lincoln (1991), but the edge length of pentagons was 2.0 nm.

(3) Pentagon subunits have recently been found in many crystalline phases coexisting with quasicrystals. In orthorhombic phases, such as Al_3Mn/Al_4Mn (Kang, Malaman, Venturini & Dubois, 1992; Li, Shi & Kuo, 1992; Hiraga, Kaneko, Matsuo & Hashimoto, 1993; Shi, Li, Ma & Kuo, 1994), Al_3Co (Li, Ma & Kuo, 1994) or the orthorhombic $Al_{13}Co_4$ (Grin, Burkhardt & Ellner, 1994), and several Al–Cr–Fe phases (Dong, Dubois, Kang & Audier, 1992), the lattice parameters in the pentagonal layers can be recovered from the decagonal quasilattice constant by substituting a *rational* ratio of

two consecutive Fibonacci numbers as an approximant for the *irrational* τ in the quasicrystals (Zhang & Kuo, 1990; Kuo, 1993). Therefore, these crystalline phases are called approximants of a decagonal quasicrystal. Pentagons also exist in hexagonal crystals, such as the μ-Al_4Mn phase (Shoemaker, 1993), and this had been discussed together with the structural model of the Al–Mn decagonal quasicrystal.

The authors wish to thank the Chinese Academy of Sciences and the National Natural Science Foundation of China for financial support. XZL is also grateful to the Postdoctoral program of China for a grant.

References

BARBIER, J.-N., TAMURA, N. & VERGER-GAUGRY, J. L. (1993). *J. Non-Cryst. Solids*, **153**, **154**, 126–131.

BLACK, P. J. (1955*a*). *Acta Cryst.* **8**, 43–48.

BLACK, P. J. (1955*b*). *Acta Cryst.* **8**, 175–182.

DONG, C., DUBOIS, J. M., KANG, S. S. & AUDIER, M. (1992). *Philos. Mag. B*, **65**, 107–126.

GRIN, J., BURKHARDT, U. & ELLNER, M. (1994). *J. Alloys Comp.* **206**, 243–247.

GRÜNBAUM, B. & SHEPHARD, G. C. (1987). *Tiling and Patterns*. San Francisco: Freeman.

HENLEY, C. L. (1985). *J. Non-Cryst. Solids*, **75**, 91–96.

HIRAGA, K., KANEKO, M., MATSUO, Y. & HASHIMOTO, S. (1993). *Philos. Mag. B*, **67**, 193–205.

HIRAGA, K., SUN, W. & LINCOLN, F. J. (1991). *Jpn. J. Appl. Phys.* **30**, L302–L305.

HUDD, R. C. & TAYLOR, W. H. (1962). *Acta Cryst.* **15**, 441–442.

KANG, S. S., MALAMAN, B., VENTURINI, G. & DUBOIS, J. M. (1992). *Acta Cryst.* B**48**, 770–776.

KUMAR, V., SAHOO, D. & ATHITHAN, G. (1986). *Phys. Rev. B*, **34**, 6924–6932.

KUO, K. H. (1993). *J. Non-Cryst. Solids*, **153/154**, 40–44.

LI, X. Z., MA, X. L. & KUO, K. H. (1994). *Philos. Mag. Lett.* **70**, 221–229.

LI, X. Z., SHI, D. & KUO, K. H. (1992). *Philos. Mag. B*, **66**, 331–340.

LI, H. L., ZHANG, Z. & KUO, K. H. (1994). *Phys. Rev. B*. In the press.

MA, X. L. & KUO, K. H. (1992). *Metall. Trans A*, **23**, 1121–1128.

MA, X. L. & KUO, K. H. (1994). *Metall. Mater. Trans. A*, **25**, 47–56.

MA, X. L. & KUO, K. H. (1995). *Metall. Mater. Trans A*. In the press.

PENROSE, R. (1974). *Bull. Inst. Math. Appl.* **10**, 266–271.

SHI, N. C., LI, X. Z., MA, Z. S. & KUO, K. H. (1994). *Acta Cryst.* B**50**, 22–30.

SHOEMAKER, C. B. (1993). *Philos. Mag. B*, **67**, 869–881.

STEURER, W. & KUO, K. H. (1990). *Acta Cryst. B*, **46**, 703–712.

TSUCHIMORI, M., ISHIMASA, T. & FUKANO, Y. (1992). *Philos. Mag. B*, **66**, 89–108.

ZHANG, H. & KUO, K. H. (1990). *Phys. Rev. B*, **42**, 8907–8914.

Acta Cryst. (1995). B**51**, 43–47

Single-Crystal Pulsed Neutron Diffraction Structure of the Antiferromagnet $K_2[FeCl_5(H_2O)]$ With and Without Applied Pressure*

BY ARTHUR J. SCHULTZ

Intense Pulsed Neutron Source, Argonne National Laboratory, Argonne, IL 60439, USA

AND RICHARD L. CARLIN

Department of Chemistry, The University of Illinois at Chicago, Chicago, IL 60607, USA

(*Received* 15 *February* 1994; *accepted* 18 *July* 1994)

Abstract

The crystal structure of $K_2[FeCl_5(H_2O)]$ was examined at 15 K and ambient pressure (1 bar = 0.1 MPa) and at 15 K and 0.14 GPa (1.4 kbar) by single-crystal time-of-flight neutron diffraction in order to search for structural changes coincident with the discontinuity in the slope of the spin-flop transition field (H_{SF}) *versus* pressure at 60 MPa. It is found that intramolecular and hydrogen-bond distances and angles are statistically equivalent at the two pressures. However, there are significant changes of as much as 0.049 (3) Å in the intramolecular Cl···Cl distances which may affect the Fe—Cl···Cl—Fe superexchange pathways and the discontinuity in H_{SF}. Dipotassium aquapentachloroferrate(III), M_r = 329.3, $F(000)$ = 636, orthorhombic, *Pnma*, Z = 4. At 15 K and ambient pressure (0.1 MPa), a = 13.452 (5), b = 9.631 (2), c = 7.003 (2) Å, V = 907.3 (5) Å^3, D_x = 2.41 g cm^{-3}. At 15 K and 0.14 GPa, a = 13.391 (4), b = 9.648 (2), c = 6.942 (2) Å, V = 896.9 (4) Å^3, D_x = 2.44 g cm^{-3}. The a and c axes decrease slightly, whereas the b axis increases slightly, under applied pressure.

* The author of this manuscript is a contractor of the US Government under contract No. W-31-109-ENG-38. Accordingly, the US Government retains a non-exclusive, royalty-free license to publish or reproduce the published form of this contribution, or allow others to do so, for US Government purposes.

Introduction

The series of compounds $A_2[FeX_5(H_2O)]$ (A = K, Rb, Cs, and NH_4; X = Cl and Br) have been extensively